Thermodynamics and Kinetic Studies for the Adsorption Process of Methyl Orange by Magnetic Activated Carbons

Authors: Cordova Estrada, Ana Karen, Cordova Lozano, Felipe, and Lara Díaz, René Alejandro

Source: Air, Soil and Water Research, 14(1)

Published By: SAGE Publishing

URL: https://doi.org/10.1177/11786221211013336

Thermodynamics and Kinetic Studies for the Adsorption Process of Methyl Orange by Magnetic Activated Carbons

Air, Soil and Water Research
Volume 14: 1–11
© The Author(s) 2021
Article reuse guidelines:
sagepub.com/journals-permissions
DOI: 10.1177/11786221211013336

Ana Karen Cordova Estrada[1], Felipe Cordova Lozano[3] and René Alejandro Lara Díaz[2]

[1]Departament of Civil and Engineering, Universidad de las Américas Puebla UDLAP, San Andrés Cholula, Puebla, México. [2]School of Engineering, Universidad de las Américas Puebla UDLAP, San Andrés Cholula, Puebla, México. [3]Department of Chemistry and Biological Sciences, Universidad de las Américas Puebla, San Andrés Cholula, Puebla, México

ABSTRACT: This study investigates the adsorption behavior of methyl orange (MO) by magnetic activated carbons (MACs) with different ratios of AC: Magnetite from aqueous solution. Batch experiments for MO adsorption were carried out for evaluating the thermodynamics and kinetics parameters onto the MAC adsorbents. Variables such as pH, initial concentration of the dye, contact time, and temperature have been analyzed. The physicochemical characteristics of MACs were analyzed by scanning electron microscopy (SEM), surface area analyzer (BET), and X-ray power diffraction. The results of SEM and BET analysis showed that MAC adsorbents present a porous structure and large surface area, suitable conditions for the adsorption process. The X-ray diffraction patterns of MACs revealed that the adsorbents possess magnetite as magnetic material. Adsorption kinetic studies carried out onto MACs showed that the pseudo-second-order model provides a good description of the kinetic process. The adsorption equilibrium results were well adjusted to the Langmuir isotherm, showing that the maximum adsorption capacity was for MACs with a ratio 3:1 and 2:1 AC/magnetite. Thermodynamic analysis declares that the adsorption process was established as spontaneous, endothermic, and physical adsorption in nature. The results of the this study indicated that MAC adsorbents can be used successfully for eliminating MO from aqueous solution.

KEYWORDS: activated carbon, adsorption kinetics, magnetic composite, methyl orange

TYPE: Original Research

CORRESPONDING AUTHOR: Felipe Cordova Lozano, Department of Chemistry and Biological Sciences, Universidad de las Américas Puebla (UDLAP), Ex-Hacienda de Santa Catarina Mártir S/N, San Andrés Cholula 72810, Puebla, México.
Email: Felipe.cordova@udlap.mx

Background

The increasing activity of the industrial process has accelerated the contamination of water resources, which has become one of the most important challenges to solve in the world. Many industries such as textile, clothing, printing, leather, paper, food, pharmaceutical, among others, use dyes for their process, which are discharged directly to the receiving water bodies at different concentrations without waste treatment. This discharge causes negative effects to the environment (De Luca et al., 2019) and human health such as aesthetic problems, high biotoxicity, and potential mutagenic and carcinogenic problems (Filippo et al., 2015).

One of the most commonly used dyes in industry is methyl orange (MO), an acidic/anionic dye with one azo group in its chemical structure, which is light resistance and non-biodegradable, with toxic, mutagenic, and carcinogenic properties which represent a serious problem for aquatic systems. The pollution of water sources by MO is mainly anthropogenic and is associated principally with the textile, printing, and food industries (Chaukura et al., 2017; Chen et al., 2011). The presence of dyes in water is undesirable because it prevents the penetration of light that is essential for living of aquatic ecosystems and can also reach irrigation systems of agricultural products for human consumption (Chung et al., 1981; Ramírez-Llamas et al., 2015). Moreover, acute exposure to this hazard dye can cause shock, vomiting, heart rate, and tissue necrosis in humans (Gong et al., 2013; Haque et al., 2011). Thus, it is important to remove this dye from wastewaters.

There are different processes for the removal of MO that include physical, chemical, and biological processes. Specifically, some electrochemical techniques, advanced oxidation process, and photochemical degradation methodologies have been used for removing MO from wastewater effluents (El-Sayed et al., 2018; Iqbal et al., 2011; Yagub et al., 2014). However, these techniques have the drawback of being demanding in time-consuming and cost. To overcome this drawback, adsorption process has become a most effective method to remove dyes from wastewater, which has been used both in laboratory batch experiments and in industrial processes for the separation and elimination of dyes and organic contaminants contained in effluents (Al-qodah, 2000). The principal advantage is its low cost and facile adaptation. An important variety of adsorbent materials that have been applied for removing of contaminants from contaminated water sites are carbons materials (Huang et al., 2017; Pal et al., 2013). Granular and powdered activated carbon (GAC, PAC) are adsorbents mainly used for adsorption processes due to its physicochemical characteristics (large surface area, porous structure, and various functional groups to adsorb colored dyes) and its low cost (Rattanapan et al., 2017; Sivashankar et al., 2014). However, these common adsorbents are difficult to recover from the liquid phase after having reached a saturated adsorption, especially the PAC,

representing a challenging for the process (Hasan & Hammood, 2018; Juang et al., 2018). Centrifugation and filtration are usually adapted to separate the used PAC from liquid solutions; however, both methods are costly and required more time to treat the wastewater. Therefore, more research is required to recover the saturated PAC from aqueous environment (Nakahira et al., 2006; Van et al., 2019).

To achieve this goal, there are many studies that prove magnetic separation as a non-energy consumption technology that can be used to recover the magnetic adsorbent. This magnetic separation process is carried out by applying a magnetic external field to the ferromagnetic materials providing a low cost, easy separation, and high efficiency technique for extracting these magnetic adsorbents (Fard & Barkdoll, 2019).

The combination of magnetic iron oxide (Fe_3O_4) and AC (Kakavandi et al., 2013) affords an attractive composite material with unique characteristics as adsorbent magnetic material (Rocher et al., 2008). Recently, magnetic activated carbons (MACs) have become a class of magnetic adsorbents for removing organic compounds, which provides a low cost material with simple implementation and recuperation (Gholamvaisi et al., 2014; Oliveira et al., 2002). However, MACs will have a disadvantage related to the pore space—it may be occupied by the magnetic nanoparticles, reducing its surface area (Juang et al., 2018). Therefore, the main objective of this study was to evaluate the synthesis with different ratios AC:Fe_3O_4 nanoparticles and its application as a magnetic adsorbent (MAC) to remove MO from aqueous solution in terms of its adsorption equilibrium, kinetics, and thermodynamics to understand the mechanism of adsorption of MO molecules onto MACs.

Materials and Methods

Chemical and instruments

All the components were analytical reagent-grade. AC powder was purchased from Hycel Co. Ferric chloride ($FeCl_3$) and iron sulfate ($FeSO_4$) were purchased from Merck. Sodium hydroxide (NaOH) and the MO ($C_{14}H_{14}N_3NaO_3S$) were purchased from Sigma-Aldrich Co. For the measure of pH solution, we used a Crison pH-meter (GLP22), and for the MO concentrations at initial, at time *t*, and equilibrium conditions, we used a UV-Visible spectrophotometer (Varian Cary 100 UV-Vis Spectrophotometer). For the magnetic separation of the adsorbent from aqueous solution, we used a magnetic neodymium disk with an intensity of 1.3T.

Preparation of MACs

The MACs with different ratios were synthesized by a chemical co-precipitation method according to the methodology established by Furlan and Melcer (2014) and Do et al. (2011). At first, in a volume of 400 mL of deionized water (DI), different amounts of AC (3.3, 6.6, and 9.9 g) were dispersed separately and heated at 80°C for 1 hr. Subsequently, 7.8 g of $FeCl_3$ and 3.9 g of $FeSO_4$ were added and stirred at 80°C for 2 hr. A solution of 5 M of NaOH was added dropwise to this suspension with continuous stirring, to precipitate the iron oxide. After adding the NaOH solution, the color of the mixture was ripped to black. To remove some impurities, the MACs were washed with 0.05 M HCl solution, sonicated twice, and finally washed several times with DI water until obtaining a neutral pH. Finally, the MAC with different ratios of AC/magnetite (1:1, 2:1 and 3:1) was separated by a neodymium disk magnet, dried at 110°C for 6 hr and kept in a desiccator until use.

Characterization of adsorbents

The specific surface areas and average pore size distribution of the MACs as well as of AC were determined by Brunauer, Emmett, and Teller (BET; BELSORP Japan Inc., Japan) using the method of physical adsorption of N_2 gas at 76 K. The morphologies of adsorbents were obtained by using a field emission scanning electron microscopy (FESEM, TESCAN, MAIA 3). For the analysis of the crystalline structure of the MACs, an X-ray diffractometer (XRD) (Rigaku D. Max Ultima II, θ/θ powder diffractometer) was used with the exploration region of 2θ from 20° to 100°.

Adsorption studies

All adsorption experiments were carried out on a horizontal shaker at 150 rpm using 250 mL Erlenmeyer flasks. A series of adsorption experiments were carried out under different operating conditions related to the initial pH of the solution, the contact time, the initial concentration of the dye, and the temperature. The first experiment investigated the effect of the initial pH on the adsorption process of MO. The initial pH for MO solutions (30 mg/L) was adjusted to 2.48, 2.78, 3.86, 5.01, 6.06, and 8.00 values with 0.1 M HCl or 0.1 M NaOH solutions; an amount of 0.020 g of MAC 2:1 was added to each MO solution in the stoppered flask and then stirred horizontally for 2.5 hr at 150 rpm (298.15 K). The second experiment studied the effect of contact time to determine the equilibrium time of MO adsorption. An amount of 0.02 g of MACs was dispersed in 100 mL of MO solution (30 mg/L, pH = 2.78) and stirred horizontally (150 rpm) at temperatures of 293.15, 298.15, 303.15 and 308.15 K during contact times ranging from 5 to 150 min. The third experiment consisted of studying the adsorption isotherms, where 100 mL of MO solution were prepared at different initial concentrations of MO ranging from 1.0 to 40 mg/L (pH = 2.78), adding 0.02 g of MACs and at equilibrium time. This experiment was also performed at all temperatures (293.15–308.15 K). The concentration of MO in the suspended solution was measured using a UV-Vis spectrophotometer at the wavelength corresponding to the maximum absorbance for MO (506 nm).

Adsorption kinetics

The amount of MO adsorbed q_t (mg/g) at time *t* (min) was calculated from Equation 1:

$$q_t = \frac{V(C_0 - C_t)}{m}, \quad (1)$$

where C_0 and C_t are MO concentrations (mg/L) at initial and t time, respectively, V (L) is the volume of the MO solution, and m is the mass of the adsorbent. The removal percentage could be calculated using Equation 2:

$$\%\,\text{removal} = \frac{(C_0 - C_t)}{C_0} \times 100. \quad (2)$$

Adsorption isotherms

The adsorption isotherms describe the equilibrium relationship between the adsorbate in solution and in the adsorbent at constant temperature. The obtained parameter from isotherms provides significant information about the adsorption mechanism and efficiencies of the adsorbent for the removal of dye (Darwish et al., 2019). The amount of the adsorbed MO at equilibrium condition (q_e) (mg/g) on MACs was calculated from the following Equation 3 (Umpuch & Sakaew, 2013):

$$q_e = \frac{V(C_0 - C_e)}{m}, \quad (3)$$

where C_0 (mg/L) is the initial concentration of MO and C_e (mg/L) is the concentration of MO at equilibrium state in aqueous phase. The Langmuir isotherm represented by Equation 4 expresses a monolayer formation of MO molecules on the adsorbent surface with a finite number of active sites equivalents in energy (Langmuir, 1918):

$$q_e = \frac{q_{\max} K_L C_e}{1 + K_L C_e}, \quad (4)$$

where $q_{\max}$ (mg/g) is the maximum adsorption capacity corresponding to the complete coverage of the monolayer on the surface of the adsorbent and K_L is the Langmuir constant (L/mg) related to equilibrium adsorption. Equation 4 can be expressed in a linear relationship if the adsorption process fits to the Langmuir model (Equation 5):

$$\frac{C_e}{q_e} = \frac{1}{K_L q_{max}} + \frac{C_e}{q_{max}}. \quad (5)$$

The essential characteristics of the Langmuir isotherm can be expressed in terms of a factor known as "R_L," a dimensionless constant called the separation factor, defined as expressed in Equation 6 (Juang et al., 2018):

$$R_L = \frac{1}{1 + K_L C_0}. \quad (6)$$

This parameter suggests the type of isotherm, where there are four possibilities according to the value of R_L: (1) if $0 < R_L < 1$, the process is favorable; (2) if $R_L > 1$, the process is unfavorable; (3) if $R_L = 1$, the process is a linear sorption; and (4) if $R_L = 0$, the process is irreversible.

Other important isotherm model for describing the mechanism of adsorption process is Freundlich isotherm, which principally describes a multisite adsorption with a heterogeneous surface (Sparks, 2003). The equation for this isotherm is expressed as follows:

$$q_e = K_F C_e^{1/n}, \quad (7)$$

where K_F is the Freundlich isotherm constant (mg g^{-1} [mg $L^{-1}]^n$), n is an indicator of the adsorption effectiveness, and q_e and C_e have the same meaning as mentioned before. The constant n gives an idea of the adsorption intensity, so high n values indicate a relatively uniform surface, whereas low values mean high adsorption at low solution concentrations. The linear form of Equation 8 allows to calculate the K_F and n values:

$$\ln q_e = \ln K_F + \frac{1}{n} \ln C_e. \quad (8)$$

Adsorption thermodynamics

The effect of temperature and thermodynamics parameter (ΔG°, ΔH°, ΔS°) for adsorption of MO on MAC was evaluated. The thermodynamic parameters are essential to better understand the effect of temperature on the adsorption process, indicating whether processes occur spontaneously. These parameters include the change in enthalpy (ΔH°), entropy (ΔS°), and Gibbs free energy (ΔG°). The values of ΔH° and ΔS° were estimated from the slope and the intercept of the Van't Hoff graph represented as ln K_C versus $1/T$ based on Equation 9. The value of ΔG° is determined from Equation 10 (Darwish et al., 2019):

$$\ln K_C = \frac{\Delta S^\circ}{R} - \frac{\Delta H^\circ}{RT}, \quad (9)$$

$$\Delta G^\circ = -RT \ln K_C, \quad (10)$$

where R (8.314 J/mol K) is the universal gas constant, K_C is the equilibrium constant, and T (K) is the absolute temperature of the solution.

Results and Discussion

Adsorbent characterization

BET surface area and porosity. The specific surface areas of the adsorbents and pore size distribution were measured by the BET method. The BET values were obtained a monolayer equivalent of the surface area (S_{BET}). The results show that the MAC adsorbents reduce its specific surface area, for example, for AC and MAC 1:1, the specific surface area decreases from 616.04 to 236.20 m^2 g^{-1}. The differences in specific surface areas between

Table 1. BET Parameters for AC and MACs Adsorbents.

ADSORBENT	S_{BET} (M^2 G^{-1})	V_P (CM^3 G^{-1})	PORE DIAMETER (NM)
CA	616.04	0.6857	4.4520
MAC 3:1	281.62	0.3975	5.6453
MAC 2:1	267.85	0.4335	6.4743
MAC 1:1	236.20	0.4057	6.8703

AC:activated carbon; MAC:magnetic activated carbon.

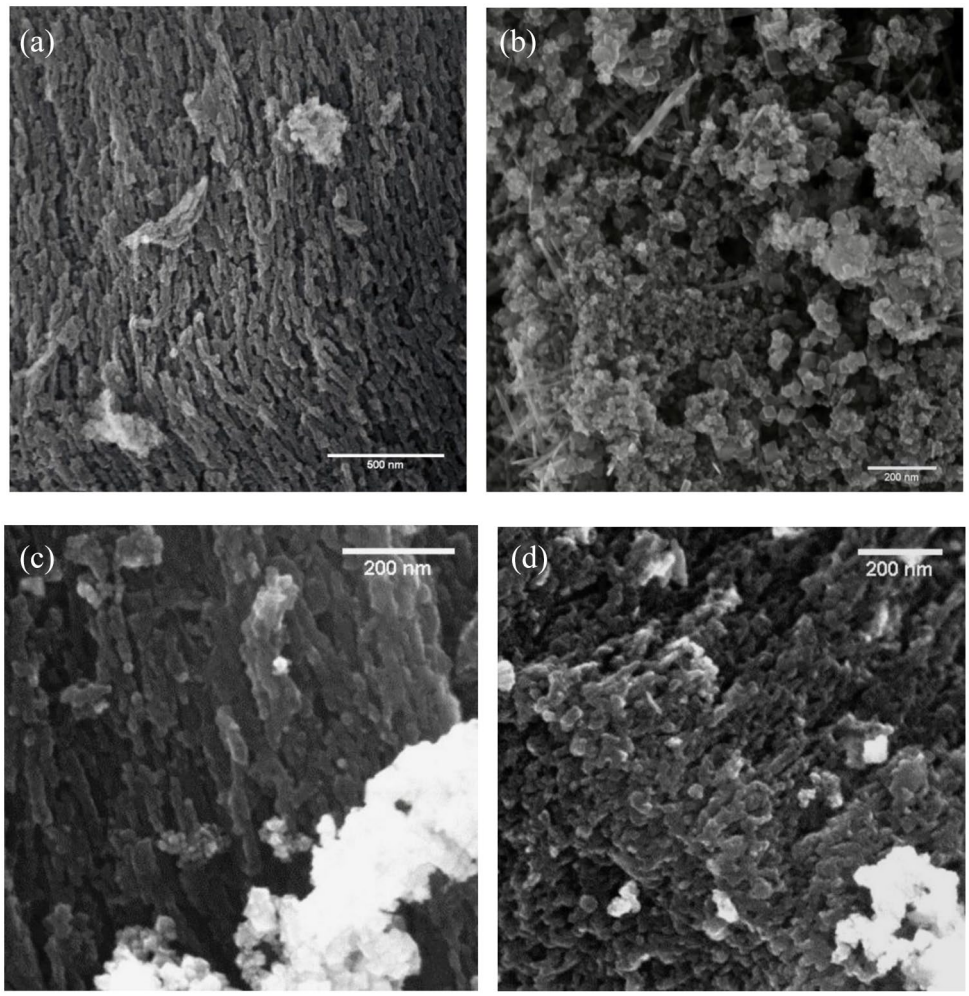

Figure 1. FESEM images showing the morphologies of (a) AC powder and MACs adsorbents with different AC ratios, (b) 1:1, (c) 2:1, and (d) 3:1.
FESEM: field emission scanning electron microscopy; AC:activated carbon; MAC:magnetic activated carbon.

AC and MACs are due to the occupation of active sites by magnetite into the porous structure of AC that blocks active sites for the adsorption of N_2, thus reducing the specific surface area. Rodrigues et al. (2020) report similar values for MAC. Table 1 shows the different parameter from BET analysis.

Scanning electron microscopy. Figure 1 shows surface morphologies for AC and MACs obtained by field emission scanning electron microscopy (FESEM). The images were obtained from 98 to 250 k× magnifications. Figure 1(b), (c), and (d) show that MACs present nanoparticles (Fe_3O_4) onto the surface of AC. The amount of the Fe_3O_4 nanoparticles in the MACs decreases significantly as the weight ratio of the AC increases in the MAC adsorbents. The porous structure of activated carbon (Figure 1(a)) was modified due to the presence of magnetic nanoparticles; however, for adsorbents with a 2:1 and 3:1 AC ratio, there is still an excellent porosity which is in beneficial for its adsorption capacity for these adsorbents, moreover of their magnetic properties necessary for separating it from the liquid medium.

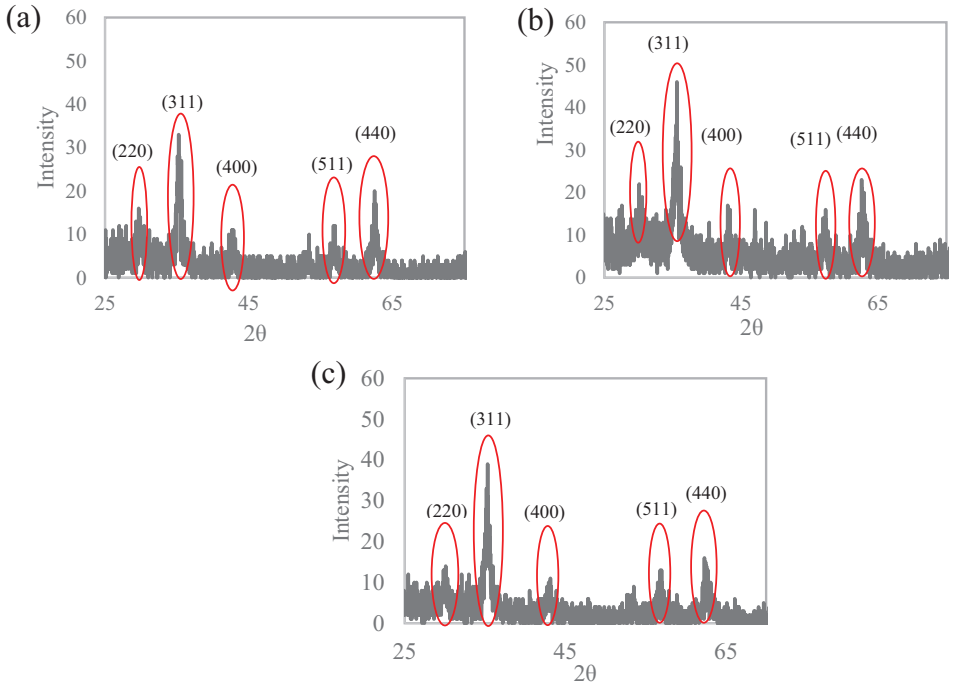

Figure 2. XRD pattern of (a) MAC 1:1, (b) MAC 2:1, and (c) MAC 3:1.
XRD: X-ray diffractometer; MAC: magnetic activated carbon.

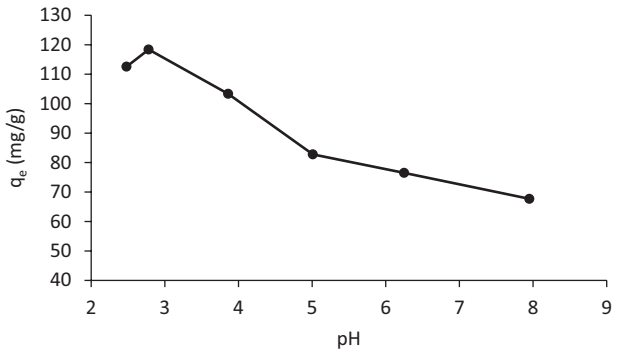

Figure 3. Effect of initial pH solution on the adsorption capacity of MO onto MAC 2:1. The MO concentration was fixed at 30 ppm for each pH solution and the amount of MAC 2:1 was 0.02 g.
MO: methyl orange; MAC: magnetic activated carbon.

XRD analysis. The XRD patterns of MAC 1:1, 2:1, and 3:1 were analyzed in a range of 20°–80° (2θ), with lapses of 0.02°–0.04° (2θ). Figure 2 shows the characteristic peaks of Fe_3O_4, and these peaks are according with that reported by Van et al. (2019). These 2θ peaks of MAC 1:1 (Figure 2(a)) = 29.9°, 35.13°, 42.89°, 56.70°, and 62.65° indicate Fe_3O_4 reflections of (220), (311), (400), (511), and (440); these results indicate a cubic crystal structure of Fe_3O_4, according to JCPDS No. 82-1533. This also indicates that no other crystalline phases are formed in the MAC adsorbents and that the Fe_3O_4 nanoparticles are bound to the AC powders are pure (Gholamvaisi et al., 2014). For the MAC 2:1 and 3:1 (Figure 2(b) and (c)), it is observed that both the intensity peaks remain stable and the crystallographic structure. This indicates that although there is a reduction in proportion of the magnetite, it remains stable on the surface of the AC. Based on the XRD-obtained pattern, the composite of AC and magnetite was confirmed and the crystallite size average of Fe_3O_4 was found to be 14.68 nm for MAC 1:1, 10.46 nm for MAC 2:1, and 12.27 nm for MAC 3:1; determined by Scherrer equation.

Effect of pH. The pH values play an important role in the adsorption process because this parameter influences both the surface properties of the MACs adsorbents and the dissociation process of the MO molecules in aqueous media. To evaluate the influence of pH on the adsorption capacity of MACs, experiments were carried out at initial MO concentration of 30 mg/L and pH range from 2.48 to 8.0. Figure 3 shows the influence of the pH on the adsorption capacity of MAC 2:1. It is observed that as the pH value increases from 2.78 to 5.0, the adsorption capacity of MAC 2:1 for the adsorption of the dye rapidly decreases from 118.4 to 82.8 mg/g. Then, a slow decrease was observed from 82.8 to 67.7 mg/g with an increase in the pH from 5.0 to 8.0. The decreasing adsorption at higher pH values is due to the abundance of OH^- ions in the aqueous media and also for the ionic repulsion between the negatively charged surface of MAC and the anionic MO molecules (Hameed et al., 2007). At low pH values, the surface of the MAC adsorbents are positively charged increasing the electrostatic attractions between its surface and the negatively charged MO anions causing an increase in the adsorption capacity. However, if the pH condition is strongly acidic, there is electrostatic repulsion between protonated MO and the positively charged active surface of MAC. It can be concluded that the optimum pH for adsorption process of MO is 2.78 and this

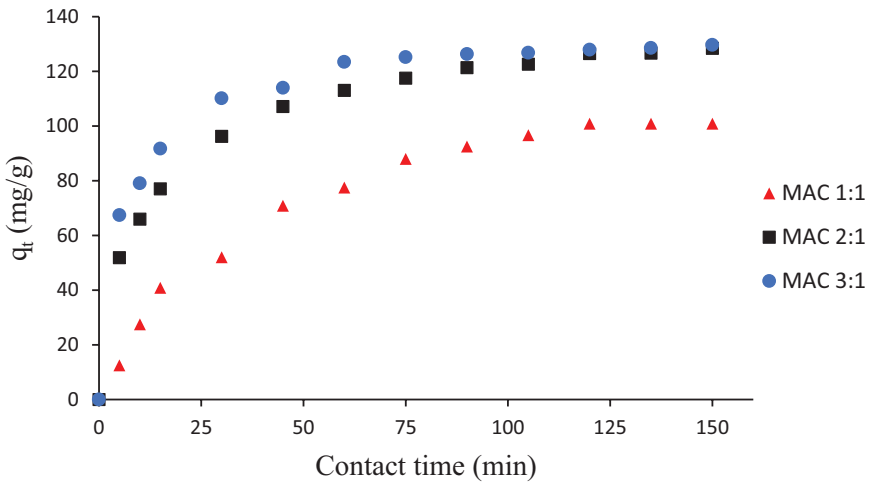

Figure 4. The variation of adsorption capacity with adsorption time at 293.15 K. The initial concentration of MO was 30 mg/L (100 mL). The different adsorbents were MACs 1:1, 2:1, and 3:1. All solutions contain 0.02 g of adsorbents.
MO: methyl orange; MAC: magnetic activated carbon.

pH value is used for the rest of experiments. Similar result has been obtained by Domga et al. (2016), for the adsorption process of MO on activated carbon obtained from Gudali bones.

Effect of contact time. The time required to attain the state of equilibrium is termed equilibrium time, and the amount of dye adsorbed at the equilibrium time reflects the maximum adsorption capacity of the adsorbent under those operation conditions (Hameed et al., 2007). Figure 4 represents the variation of adsorption capacity in function of adsorption time. In general, the adsorption rate was fast during the first 15 min for the magnetic adsorbents containing a high content of activated carbon, indicating that at the beginning of the adsorption process, there are a large number of active sites available from the adsorbents. The equilibrium state for MACs 2:1 and 3:1 was reached approximatively after 60 min where the percentage removal of MO is greater than 80%. This removal percentage is higher than 90% after 135 min for high content–activated carbon adsorbents. For the MAC 1:1 adsorbent, the magnetic nanoparticle bocks activate sites limiting the adsorption capacity and yielding a low percentage removal of MO (58% at 60 min).

Adsorption isotherms. The distribution of MO molecules in the liquid phase and the solid phase can be provided by isotherm parameters. In this study, the Langmuir and Freundlich isotherm models were used for the analysis of the adsorption data. As the adsorption capacity of the MAC 3:1 and MAC 2:1 adsorbents is similar, the MACs 2:1 and 1:1 adsorbents have been selected for analyzing the effect of initial concentration of MO in the adsorption process analysis. Figure 5 shows the linear graphs for the Langmuir and Freundlich adsorption isotherms and the graph for R_L values in function of initial concentration of MO for MAC 2:1 (Figure 5(a), (c), and (e)) and MAC 1:1 (Figure 5(b), (d), and (f)) at the temperature of 298 K. Figure 5(a) and (b) shows that for MAC 2:1 and MAC 1:1, MO adsorption follows Langmuir model reasonably well ($R^2 = .9966$ and $R^2 = .977$).

Table 2 shows the adsorption parameters for the same adsorbents at all the temperatures used in this study. In general and considering the correlation coefficient values (R^2), it is observed that the Langmuir isotherm fitted so well to the adsorption data, indicating that a monolayer of MO molecules is formed onto the surface of adsorbents which has an energetically homogeneous surface. The obtained values of R_L ($R_L < 1$) as a function of initial concentrations of MO have been obtained showing that the adsorption process is favorable to the equilibrium concentrations of MO. For the temperature, it is observed that as the temperature increases, the adsorption capacity of the adsorbent increases (Figure 6), revealing that the adsorption process of MO onto MACs adsorbents is endothermic in nature.

Adsorption kinetics. To obtain a better understanding on the adsorption mechanism of MO dye, the pseudo-first-order and pseudo-second-order models were used. According to Umpuch and Sakaew (2013), the pseudo-first order model is the first model that describes the adsorption rate based on adsorption capacity. The pseudo-first-order model is generally expressed by Equation 11:

$$\ln\left(q_e - q_t\right) = \ln q_e - k_1 t, \tag{11}$$

where k_1 (min^{-1}) is the pseudo-first-order rate constant and q_e and q_t are the amounts of MO adsorbed (mg/g) at equilibrium and time t (min). The pseudo second-order kinetic model proposed by Ho and McKay (1998) is expressed in a linear form by Equation 12:

$$\frac{t}{q_t} = \frac{1}{k_2 q_e^2} + \frac{t}{q_e}, \tag{12}$$

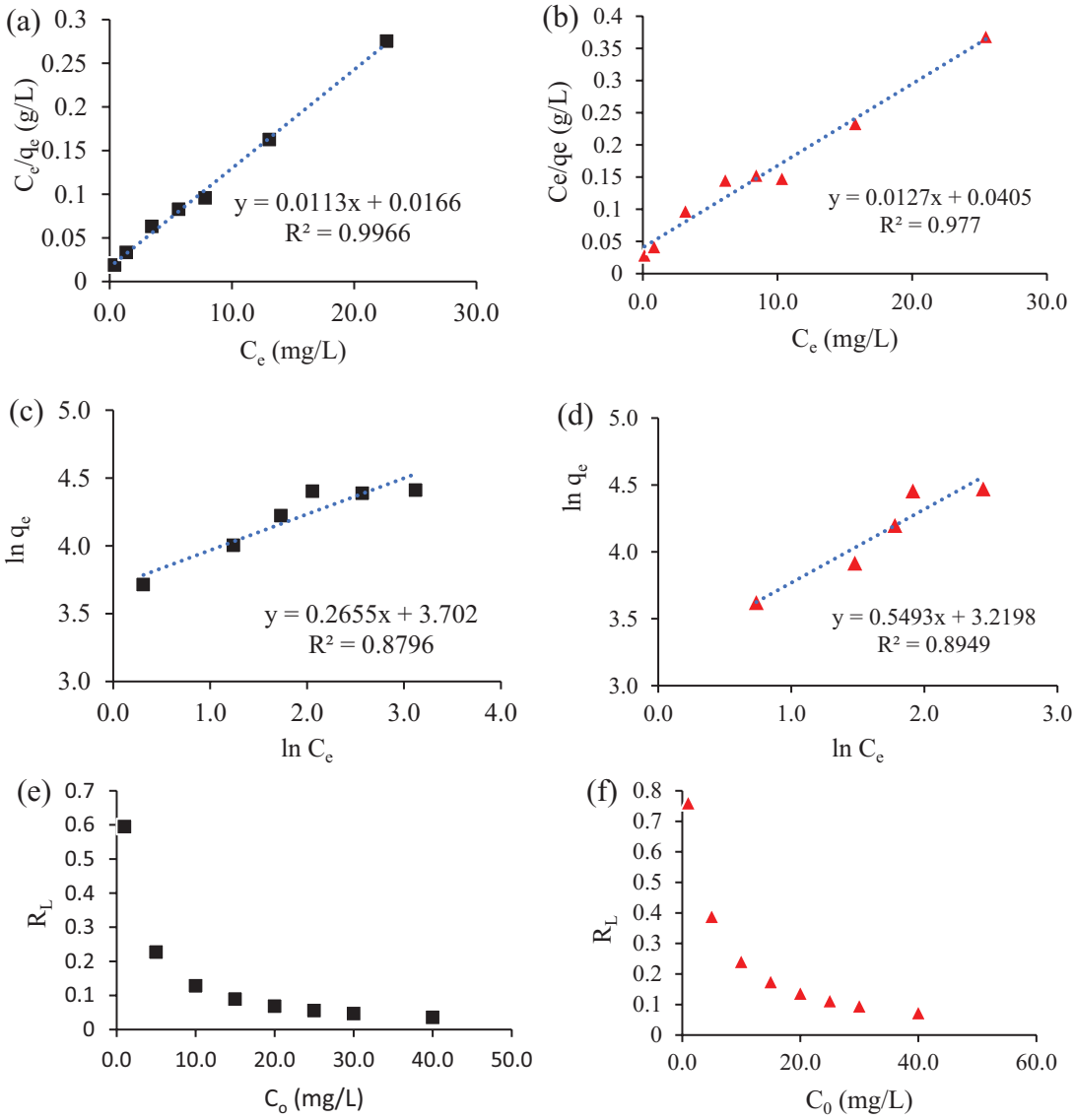

Figure 5. Langmuir and Freundlich isotherms and R_L graphs for (a, c, and e) MAC 2:1 and (b, d, and f) MAC 1:1 at 298.15 K.
MO: methyl orange; MAC: magnetic activated carbon.

Table 2. Adsorption Parameters From Langmuir and Freundlich Isotherm Models Using MAC 2:1 and 1:1 at Different Temperatures.

MODEL		*T* = 293.15 (K)		*T* = 298.15 (K)		*T* = 303.15 (K)		*T* = 308.15 (K)	
		MAC 2:1	MAC 1:1	MAC 2:1	MAC 1:1	MAC 2:1	MAC 1:1	MAC 2:1	MAC 1:1
Langmuir isotherm	q_{max} (mg/g)	84.00	62.50	88.50	78.74	144.93	92.59	189.2	128.2
	K_L (L/mg)	0.1510	0.5882	0.6807	0.3136	0.1769	0.1674	0.1095	0.1483
	R^2	.9896	.9875	.9966	.977	.9688	.9336	.9689	.9937
Freundlich isotherm	K_F ((mg g^{-1}/(mg $L^{-1})^{1/n}$)	14.32	27.35	40.528	25.02	28.04	22.33	23.18	14.75
	n	1.924	1.923	3.770	1.820	1.946	2.543	1.606	1.410
	R^2	.9328	.8976	.8796	.8949	.9671	.8263	.9558	.935

MAC: magnetic activated carbon.

where k_2 (g/[mg.min]) is the pseudo-second-order rate constant and q_e and q_t have the same meaning mentioned above. Figure 7 shows the variation of adsorption capacity in function of time at different temperatures: 293.15 K (Figure 7(a)), 298.15 K (Figure 7(b)), 303.15 K (Figure 7(c)), and 308.15 K (Figure 7(d)). These results show that the adsorption capacity increased as the adsorption time increased.

Figure 8(a) to (d) shows the linear graphs for the pseudo-second-order model for MACs 2:1 and 1:1 at different temperatures. It can be seen a good linearity in these graphs with a high correlation coefficient values ($R^2 \simeq 1.0$) at all temperatures indicating that the pseudo-second-order model was more suitable for describing the adsorption kinetics of MO adsorption. For this model, it is assumed that the rate-controlling step might be chemical adsorption.

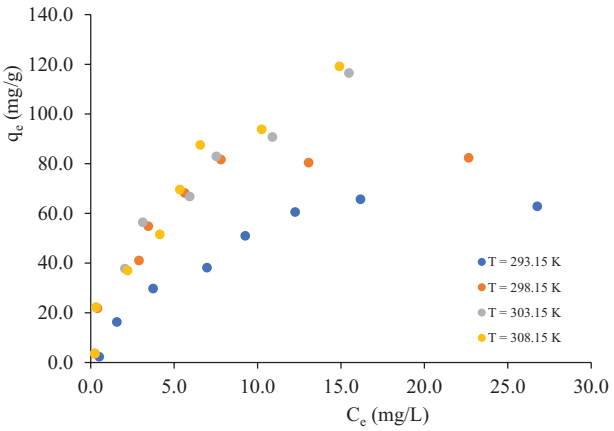

Figure 6. Adsorption isotherm and effect of temperature on the adsorption of MO on MAC 2:1: (a) 293.15 K, (b) 298.15 K, (c) 303.15 K, and (d) 308.15 K.
MO: methyl orange; MAC: magnetic activated carbon.

Activation energy. To deduce the apparent activation energy, it is possible to use the pseudo-second-order rate constant (k_2) for getting an idea of the adsorption behavior at different temperatures, using the Arrhenius equation (Equation (13)):

$$\ln k_2 = \ln A - \frac{E_a}{RT}, \tag{13}$$

where E_a is the activation energy (kJ/mol), k_2 is the pseudo-second-order rate constant for adsorption (g/[mol s]), A is the temperature-independent Arrhenius factor (g/[mol s]), R is the universal gas constant (8.314 J/[K mol]), and T is the temperature of the solution (K). According to Equation 13, the slope of the graph of ln k_2 versus $1/T$ can be used to evaluate the activation energy (E_a). Figure 9 represents the Arrhenius plots for MAC 2:1 (Figure 9(a)) and MAC 1:1 (Figure 9(b)).

From the slope of each graph, the activation energy values of 33.86 and 10.08 kJ/mol are obtained for MAC 2:1 and MAC 1:1, respectively. Considering that the obtained activation energy values are lower than 40 kJ/mol, the adsorption process of MO on MAC may include both chemical adsorption and physical adsorption.

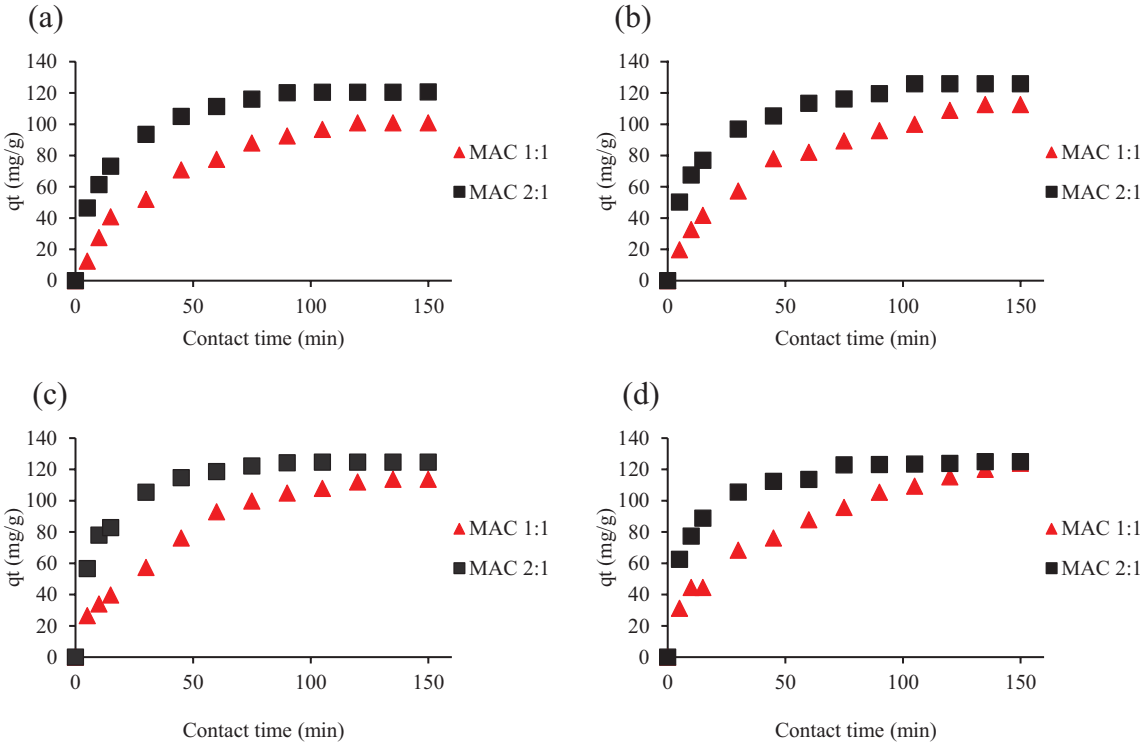

Figure 7. The variation of adsorption capacity with adsorption time at different temperatures: (a) 293.15 K, (b) 298.15 K, (c) 303.15 K, and (d) 308.15 K. The initial concentration of MO was 30 mg/L, and the amount of adsorbent was 0.02 g.
MO: methyl orange; MAC: magnetic activated carbon.

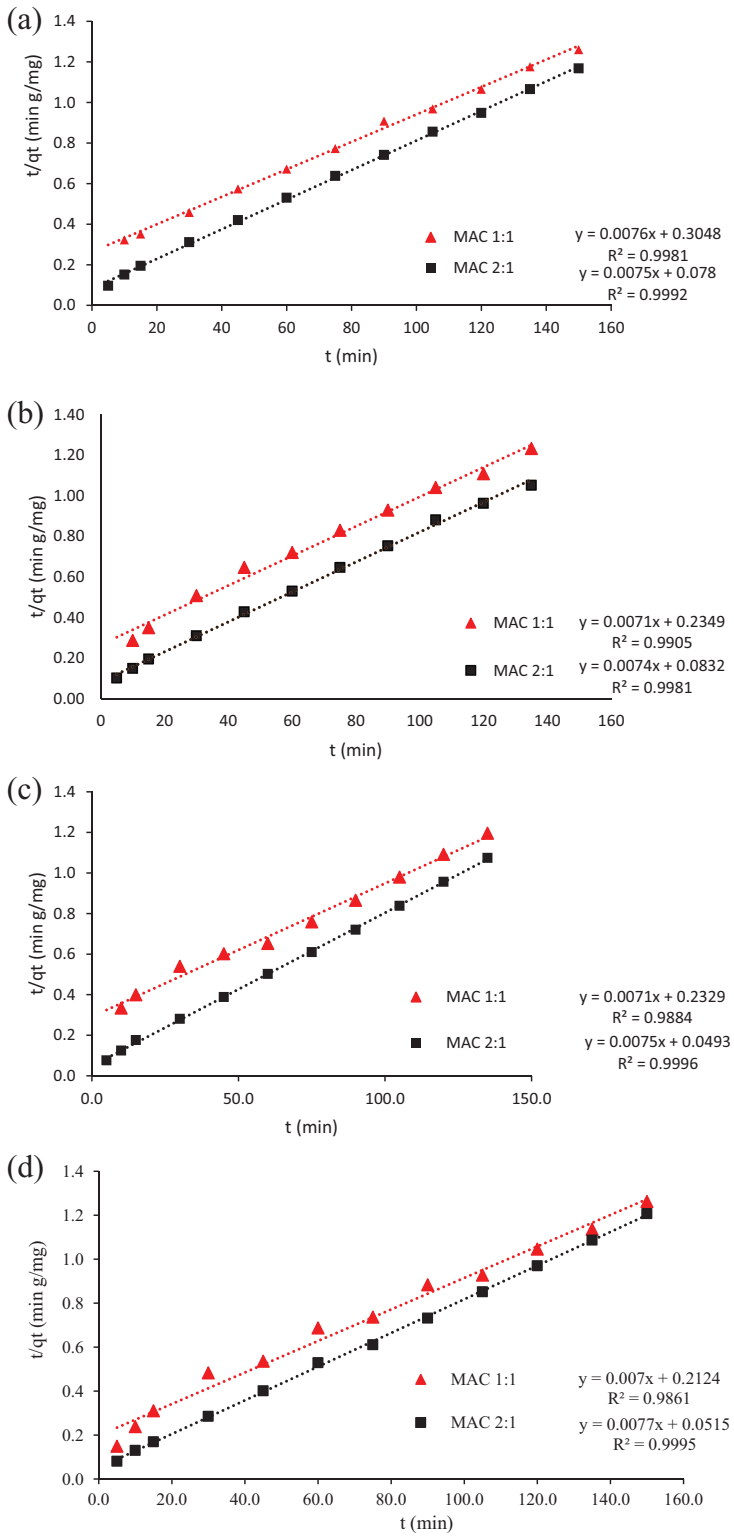

Figure 8. Linear form of the pseudo-second-order rate model of the kinetics study at different temperatures: (a) 293.15 K, (b) 298.15 K, (c) 303.15 K, and (d) 308.15 K. The initial concentration of MO was 30 mg/L, and the amount of adsorbent was 0.02 g.
MO: methyl orange; MAC: magnetic activated carbon.

Thermodynamics studies. Thermodynamic parameters were evaluated by adsorption of the MO on MAC 2:1 adsorbent in the temperature range of 293.15–308.15 K. Figure 10 shows the Van't Hoff plot for calculating the thermodynamics variables ΔS° and ΔH°. The K_C values were obtained from the isotherms at different temperatures (Figure 6).

The ΔG° values shown in Table 3 establish that the adsorption process was spontaneous at temperatures of 298.15, 303.15, and 308.15 K, which is in agreement with the ΔS° value ($\Delta S > 0$ for spontaneous process). The positive values of ΔH° implied that the adsorption process was endothermic.

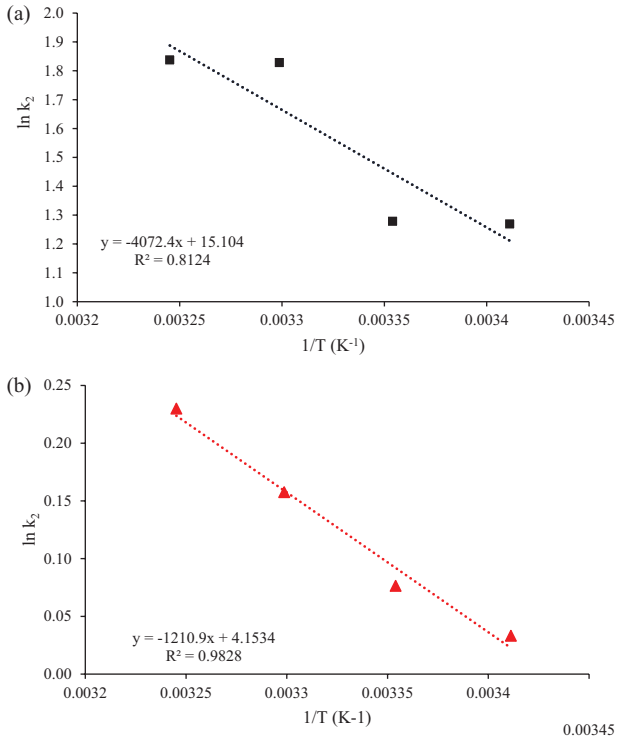

Figure 9. Plot ln k_2 versus 1/T for adsorption of MO on (a) MAC 2:1 and (b) MAC 1:1.
MO: methyl orange; MAC: magnetic activated carbon.

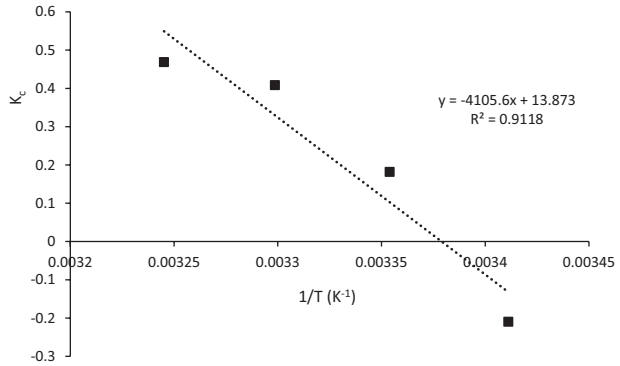

Figure 10. Van't Hoff plot for adsorption of MO onto MAC 2:1.
MO: methyl orange; MAC: magnetic activated carbon.

Table 3. Thermodynamic Parameters of MO Dye Adsorption on MAC 2:1.

TEMPERATURE (K)	K_C	$\Delta G°$ (KJ/MOL)	$\Delta H°$ (KJ/MOL)	$\Delta S°$ (J/MOL K)
MAC 2:1				
293.15	0.8107	0.511	34.14	115.34
298.15	1.199	−0.450		
303.15	1.504	−1.029		
308.15	1.597	−1.200		

MO: methyl orange; MAC: magnetic activated carbon.

Conclusion

This study shows two different adsorbents based on activated carbon that can be used as an adsorbent for the treatment of wastewater containing MO. The first one was activated carbon, which shows a big BET surface area compared with the other adsorbent. The second adsorbent was an MAC, which has very interesting properties compared with AC. One of them is that they exhibited magnetic properties and can be easily separated from the water medium by a magnetic separation. In this study, we use three different MACs (1:1, 2:1, 3:1). It demonstrates that increasing the amount of AC, the surface area it increases but the amount of magnetite it is reduced.

MACs show smaller BET surface areas compared with the AC due to the incorporation of magnetite. The presence of iron oxide in MACs was validated using XRD analysis. The SEM images proved that Fe_3O_4 particles are dispersed evenly on the surface of AC and they were nano-sized. In spite of this, the adsorption capacity of MAC is affected because of lower value compared with AC but MAC offers the possibility to be removed from water easily.

MAC 2:1 and 3:1 share similar values for adsorption capacities, so we decided to only use MAC 1:1 and MAC 2:1 to analyze their isotherms. Results demonstrate that MAC 2:1 composite was more effective in removing MO than MAC 1:1. The adsorption isotherms revealed that the adsorption fits better with Langmuir isotherm model for the adsorbents. Kinetic studies demonstrate that the adsorption data obeyed a pseudo-second-order model which is spontaneous ($\Delta G° < 0$) and endothermic ($\Delta H° > 0$) in nature.

Overall, the results demonstrate that MAC 2:1 adsorbent can be used for MO removal due to the capacity adsorption and the easily simple magnetic separation to remove pollutants from wastewater effluents. This process could have a potential application to eliminate toxic pollutants in the treatment of water contaminated with MO being of interest to the textile industries. This process could minimize environmental impacts.

Further research should include regeneration capacity of the adsorbent and the possibility to use with other organic contaminants and scaling up to a pilot study to study better the efficacy and cost.

Declaration of Conflicting Interests

The author(s) declared no potential conflicts of interest with respect to the research, authorship, and/or publication of this article.

Funding

The author(s) disclosed receipt of the following financial support for the research, authorship, and/or publication of this article: The authors are thankful for partial financial support from the Office of Graduate Programs and Research (UDLAP) and for the partial scholarship support to the PhD student Ana Karen Cordova Estrada. To Conacyt for partial scholarship support to the PhD student Ana Karen Cordova Estrada.

ORCID iDs

Ana Karen Cordova Estrada https://orcid.org/0000-0002-9569-5102

Felipe Cordova Lozano https://orcid.org/0000-0001-7517-1953

REFERENCES

Al-qodah. (2000). Adsorption of dyes using shale oil ash. *Water Research, 34*, 4295–4303. http://doi.org/10.1016/S0043-1354(00)00196-2

Chaukura, N., Murimba, E., & Gwenzi, W. (2017). Synthesis, characterisation and methyl orange adsorption capacity of ferric oxide–biochar nano-composites derived from pulp and paper sludge. *Applied Water Science, 7*, 2175–2186. http://doi.org/10.1007/s13201-016-0392-5

Chen, D., Chen, J., Luan, X., Ji, H., & Xia, Z. (2011). Characterization of anion–cationic surfactants modified montmorillonite and its application for the removal of methyl orange. *Chemical Engineering Journal, 171*, 1150–1158. http://doi.org/10.1016/j.cej.2011.05.013

Chung, K.-T., Fulk, G., & Andrews, W. (1981). Mutagenicity testing of some commonly used dyes. *Applied and Environmental Microbiology, 42*, 641–648. http://doi.org/10.1128/AEM.42.4.641-648.1981

Darwish, A., Rashad, M., & AL-Aoh, H. (2019). Methyl orange adsorption comparison on nanoparticles: Isotherm, kinetics, and thermodynamic studies. *Dyes and Pigments, 160*, 563–571. http://doi.org/10.1016/j.dyepig.2018.08.045

De Luca, P., Foglia, P., Siciliano, C., Nagy, J., & Macario, A. (2019). Water contaminated by industrial textile dye: Study on decolorization process. *Environments, 6*, 101. http://doi.org/10.3390/environments6090101

Do, M., Phan, N., Nguyen, T., Pham, T., Nguyen, V., Vu, T., & Nguyen, T. (2011). Activated carbon/Fe3O4 nanoparticle composite: Fabrication, methyl orange removal and regeneration by hydrogen peroxide. *Chemosphere, 85*, 1269–1276. http://doi.org/10.1016/j.chemosphere.2011.07.023

Domga, R., Tcheka, C., Mouthe Anombogo, G. A., Kobbe-dama, N., Tchat Chueng, J. B., Tchigo, A., & Tsafam, A. (2016). Batch equilibrium adsorption of methyl orange from aqueous solution using animal activated carbon from Gudali bones. *International Journal of Innovation Sciences and Research, 5*, 798–805.

El-Sayed, G., Hazaa, M., & El-Komy, A. (2018). Biotreatment of water polluted with methyl orange dye by using different forms of yeast. *Journal of Basic and Environmental Sciences, 5*, 217–221.

Fard, A., & Barkdoll, B. (2019). Magnetic activated carbon as a sustainable solution for removal of micropollutants from water. *International Journal of Environmental Science and Technology, 16*, 1625–1636. http://doi.org/10.1007/s13762-018-1809-5

Filippo, P. D., Pomata, D., Riccardi, C., Buiarelli, F., & Gallo, V. (2015). Oxygenated polycyclic aromatic hydrocarbons in size-segregated urban aerosol. *Journal of Aerosol Science, 87*, 126–134. http://doi.org/10.1016/j.jaerosci.2015.05.008

Furlan, P., & Melcer, M. E. (2014). Removal of aromatic pollutant surrogate from water by recyclable magnetite-activated carbon nanocomposite: An experiment for general chemistry. *Journal of Chemical Education, 91*, 1966–1970. http://doi.org/10.1021/ed500246s

Gholamvaisi, D., Azizian, S., & Cheraghi, M. (2014). Preparation of magnetic-activated carbon nanocomposite and its application for dye removal from aqueous solution. *Journal of Dispersion Science and Technology, 35*, 1264–1269. http://doi.org/10.1080/01932691.2013.843465

Gong, R., Ye, J., Dai, W., Yan, X., Hu, J., Hu, J., . . . Huang, H. (2013). Adsorptive removal of methyl orange and methylene blue from aqueous solution with finger-citron-residue-based activated carbon. *Industrial & Engineering Chemistry Research, 52*, 14297–14303. http://doi.org/10.1021/ie402138w

Hameed, B. H., Ahmad, A. A., & Aziz, N. (2007). Isotherms, kinetics and thermodynamics of acid dye adsorption on activated palm ash. *Chemical Engineering Journal, 133*, 195–203. http://doi.org/10.1016/j.cej.2007.01.032

Haque, E., Jun, J., & Jhung, S. (2011). Adsorptive removal of methyl orange and methylene blue from aqueous solution with a metal-organic framework material, iron terephthalate (MOF-235). *Journal of Hazardous Materials, 185*, 507–511. http://doi.org/10.1016/j.jhazmat.2010.09.035

Hasan, M., & Hammood, Z. (2018). Wastewater remediation via modified activated carbon: A review. *Pollution, 4*, 707–723. http://doi.org/10.22059/poll.2018.255031.430

Ho, Y., & McKay, G. (1998). Sorption of dye from aqueous solution by peat. *Chemical Engineering Journal, 70*, 115–124. http://doi.org/10.1016/S0923-0467(98)00076-1

Huang, R., Liu, Q., Huo, J., & Yang, B. (2017). Adsorption of methyl orange onto protonated cross-linked chitosan. *Arabian Journal of Chemistry, 10*(1), 24–32. http://doi.org/10.1016/j.arabjc.2013.05.017

Iqbal, J., Wattoo, F. H., Wattoo, M., Malik, R., Tirmizi, S., Imran, M., & Ghangro, A. (2011). Adsorption of acid yellow dye on flakes of chitosan prepared from fishery wastes. *Arabian Journal of Chemistry, 4*, 389–395. http://doi.org/10.1016/j.jtice.2017.12.005

Juang, R. S., Yao-Chung, Y., Chien-Shiun, L., Kuen-Song, L., Hsi-Chuan, L., Sea-Fue, W., & An-Cheng, S. (2018). Synthesis of magnetic Fe3O4/activated carbon nanocomposites with high surface area as recoverable adsorbents. *Journal of the Taiwan Institute of Chemical Engineers, 90*, 51–60. http://doi.org/10.1016/j.jtice.2017.12.005

Kakavandi, B., Jafar, A. J., Kalantary, R., Nasseri, S., Ameri, A., & Esrafily, A. (2013). Synthesis and properties of Fe3O4-activated carbon magnetic nanoparticles for removal of aniline from aqueous solution: Equilibrium, kinetic and thermodynamic studies. *Iranian Journal of Environmental Health Sciences & Engineering, 10*, 19.

Langmuir, I. (1918). Adsorption of gases on plain surfaces of glass mica platinum. *Journal of the American Chemical Society, 40*, 1361–1403. http://doi.org/10.1021/ja02242a004

Nakahira, A., Nishida, S., & Fukinishi, K. (2006). Synthesis of magnetic activated carbons for removal of environmental endocrine disrupter using magnetic vector. *Journal of the Ceramic Society of Japan, 114*, 135–137.

Oliveira, L., Rios, R., Fabris, J. D., Garg, V., & Sapag, K. (2002). Activated carbon/iron oxide magnetic composites for the adsorption of contaminants in water. *Carbon, 40*(12), 2177–2183. http://doi.org/10.1016/S0008-6223(02)00076-3

Pal, J., Kanti, M., Kumar, D., & Verma, D. (2013). Removal of methyl orange by activated carbon modified by silver nanoparticles. *Applied Water Science, 3*, 367–374. http://doi.org/10.1007/s13201-013-0087-0

Ramírez-Llamas, Jacobo-Azuara, & Martínez-Rosales. (2015). Adsorption of methyl orange in aqueous solutions onto layered double hydroxides. *Acta Universitaria, 25*, 25–34. http://doi.org/10.15174/au.2015.778

Rattanapan, S., Srikram, J., & Kongsune, P. (2017). Adsorption of methyl orange on coffee grounds activated carbon. *Energy Procedia, 138*, 949–954. http://doi.org/10.1016/j.egypro.2017.10.064

Rocher, V., Siaugue, J.-M., Cabuil, V., & Bee, A. (2008). Removal of organic dyes by magnetic alginate beads. *Water Research, 42*, 1290–1298. http://doi.org/10.1016/j.watres.2007.09.024

Rodrigues, S., Silva, M., Arriel, T., & Bianchi, M. (2020). Use of magnetic activated carbon in a solid phase extraction procedure for analysis of 2,4-dichlorophenol in water samples. *Water, Air, & Soil Pollution, 231*, 294. http://doi.org/10.1007/s11270-020-04610-1

Sivashankar, R., Sathya, A., Vasantharaj, K., & Sivasubramanian, V. (2014). Magnetic composite an environmental super adsorbent for dye sequestration—A review. *Environmental Nanotechnology, Monitoring & Management, 1*, 36–49. http://doi.org/10.1016/j.enmm.2014.06.001

Sparks, D. (2003). 5—Sorption phenomena on soils. In D. Sparks (Ed.), *Environmental soil chemistry* (2nd ed., pp. 133–186). Academic Press. http://doi.org/10.1016/B978-012656446-4/50005-0

Umpuch, C., & Sakaew, S. (2013). Removal of methyl orange from aqueous solutions by adsorption using chitosan intercalated montmorillonite. *Songklanakarin Journal of Science and Technology, 35*, 451–459.

Van, T., My, U., Hoang, S., Dai, L., Van, D., & Hoai, T. (2019). Adsorption of Ni(II) ions by magnetic activated carbon/chitosan beads prepared from spent coffee grounds, shrimp shells and green tea extract. *Environmental Technology, 41*, 2817–2832. http://doi.org/10.1080/09593330.2019.1584250

Yagub, M., Sen, K., Afroze, S., & Ang, H. (2014). Dye and its removal from aqueous solution by adsorption: A review. *Advances in Colloid and Interface Science, 209*, 172–184. http://doi.org/10.1016/j.cis.2014.04.002